Real-Time Control of Microgrids with Explicit Power Setpoints: Unintentional Islanding

Andrey Bernstein
Jean-Yves Le Boudec
Laboratory for Communications and Applications 2
École Polytechnique Fédérale de Lausanne
Lausanne, Switzerland
andrey.bernstein@epfl.ch, jean-yves.leboudec@epfl.ch

Lorenzo Reyes-Chamorro
Mario Paolone
Distributed Electrical Systems Laboratory
École Polytechnique Fédérale de Lausanne
Lausanne, Switzerland
lorenzo.reyes@epfl.ch, mario.paolone@epfl.ch

***Abstract*—We propose a method to perform a safe unintentional islanding maneuver of microgrids. The method is derived in the context of a framework for the real-time control of microgrids, called Commelec, recently proposed by the Authors. The framework uses a hierarchy of software agents that communicate with each other using a common, device independent protocol in order to define explicit power setpoints without the need of droop controllers. We show that the features of the framework allow to design a generic control method for treating unintentional islanding with the following properties. First, the method is able to choose the best candidate slack resource, based on the information obtained from the agents. Second, as the agent responsible for the grid has a global view of the network's status and its resources, it is possible to optimize the performance of the network during and after the islanding transition. Third, after the islanding maneuver it allows for the online switching of the slack resource to that with the best capabilities to face the network's needs. Finally, the method is suitable for inertia-less systems as the control is performed using explicit power setpoints and it does not rely on the frequency signal. We illustrate the benefits of the proposed method via simulation on the LV microgrid benchmark defined by the CIGRÉ Task Force C6.04.02, by comparing its performance to that of the standard droop-based method called *load drop anticipator*.**

***Index Terms*—Microgrids, decentralized control, explicit distributed optimization, power and voltage control, islanding, software agents**

I. Introduction

The trend of vast penetration of distributed energy resources (DERs, such as PV or wind farms) in low and medium voltage power networks calls for a substantial improvement in the control methods of these systems due to the two conflicting contributions of DERs. On one hand, more flexibility is added to the networks which allows for a better and more reliable operation on local scales. In particular, local power balances in low-voltage grids become possible, creating the so-called microgrids in the distribution networks. On the other hand, the high volatility of DERs can cause unpredictable reductions in the quality-of-supply. In this context, the local resilience of the system against major external disturbances (e.g., faults and blackouts) can be substantially improved if the microgrid is capable of performing *the islanding maneuver* (i.e., the disconnection from the main grid subsequent to an intentional or non-intentional decision, e.g., [7]).

Usually, the real-time control of microgrids is performed using droop controllers that react to frequency and voltage, while non real-time control decisions are taken by suitably defined management systems [8]. In this context, the strategy for an islanding maneuver relies on the availability of a classic slack resource with mechanical rotating inertia. Hence, the slack resource is normally predefined and, in case the islanding takes place when there is a large power import from the external grid, a shedding scheme may be required to avoid system collapse. Moreover, the sub-second control is not addressed directly, as it is left to the local droop controllers. The main advantages of this control strategy is its simplicity of implementation, as it relies on the fitting of few parameters, and that it inherently ensures that all droop-controlled units contribute to the power imbalance caused by the islanding. In contrast, the main disadvantages are: the ignorance of the state of the pre-selected slack, which may be very dynamic, especially for electrochemical storage devices and the use of locally-controlled shedding schemes that may trigger all non-critical loads at a given frequency threshold.

Recently, a different framework for the real-time control of active distribution networks, and in particular microgrids with little or null inertia, has been proposed in [1]. With the Commelec framework, electrical resources in the microgrid are under the control of one or several grid agents, which define explicit power setpoints in real-time (i.e., every ~ 0.1 sec). Contrary to classic strategies, this mode of operation exposes the state of all resources to the local grid controller, enabling an efficient and stable operation *without* large rotating masses. The framework is designed to be robust (i.e., it avoids the problems inherently posed by software controllers) and scalable (i.e., it easily adapts to grids of any size and complexity). It uses a hierarchical system of software agents, each responsible for a single resource (loads, generators and storage devices) or an entire subsystem (including a grid and/or a number of resources). It is abstract in the sense that it applies to all electrical subsystems and specifies their capabilities, expected behavior, and a simplified view of their internal state using a common, device-independent protocol.

Supported by the SNSF - NRP 70 "Energy Turnaround".

In this paper, our goal is to add to the Commelec real-time control framework the ability to support *unintentional islanding*. Our solution has the following features. First, the agent responsible for the grid ("Grid Agent") can use the information received from the resource agents about their internal capabilities in order to choose the slack resource adaptively. Second, as the grid agent has a global view of the network and its resources, it is possible to optimize the network quality-of-supply during and after the islanding. Third, in many modern microgrids there is little or no-inertia. Thus, the existing droop-based methods should be modified to estimate the *electrochemical inertia* that represents the current stored energy available for reacting to a power perturbation. In contrast, our method is directly applicable to inertia-less systems as the control is performed using explicit power setpoints and it does not rely on the frequency signal.

We illustrate the benefits of the proposed method via simulation on the LV microgrid benchmark defined by the CIGRÉ Task Force C6.04.02, by comparing its performance to that of the droop-based strategies tuned for inertialess systems. For this purpose, we extend the standard method called *load drop anticipator* used for networks steered by rotating machines.

II. State-of-the-Art on Microgrids Islanding

The unintentional islanding transition is the most difficult condition that can affect microgrids. The ability to cope with such a transition is key for ensuring the microgrid's resilience and dynamic performance [4]. In the following, when talking about islanding we always refer to the unintentional islanding transition. The state-of-the-art on mode transition of microgrids is mainly based on the P-f/Q-V droop controls and can be roughly divided into two categories. In the first category, rotating machines are present in the microgrid and hence there is an intrinsic inertia for reacting to the islanding transition. In the second category, most of the resources are interfaced through power converters and thus the inertia is negligible or nonexistent.

In both cases, the use of at least one device working in the *voltage source*-mode (VS) is a common practice so that it can react automatically to changes in power, while all other resources work in the *current source*-mode (CS).

The first category is well-spread in industry by acting over the governor of diesel, steam or gas based synchronous machines to modify their speed and, hence, the grid frequency. In this category the most used strategy is the Load Drop Anticipator (LDA). This method acts on the pre-selected slack unit for anticipating the maximum frequency variation that might take place after the islanding. For this purpose it needs to know the value of the inertia of the machine.

In the second category, enhanced droop control strategies are proposed. They usually rely on a well-sized storage system to cope with the worst possible disturbances in an islanding transition. In [2], the use of different VS-CS resources configuration is discussed. It is shown that a VS-control strategy can be used for limiting the current output of the resource during the islanding transition so that the microgrid can succesfully transit to the islanded mode. Load shedding is not discussed. In [6], a transition scheduler is proposed where, in case of islanding, all non-critical loads are shed and PV units can be curtailed. The method shows very good results in its dynamic performance for the case under study. Unfortunately, the proposed strategy is customized for the case study and cannot be directly extended to any generic microgrid.

As mentioned, the existing methods are based on the action of local droop controllers. To the best of our knowledge, the only exception to this approach is the Commelec framework [1], which uses *explicit control of power setpoints* on a very frequent time scale. In the next section, we describe some details of the framework that will be used subsequently in Section IV to define the corresponding islanding procedure.

III. Commelec Framework

In the Commelec framework, a software *agent* is associated with a resource (henceforth called "Resource Agent", RA), or an entire system including a grid and/or a number of devices (henceforth called "Grid Agent", GA). An example of the agents structure is shown in Figure 1 (b), where the GA at LV level (LVGA) is in charge of controlling a group of RAs responsible for specific subsystems. The agents relation corresponds to the case study shown in Figure 1 (a), which is used here to evaluate the performance of the proposed methods – see Section V for further details.

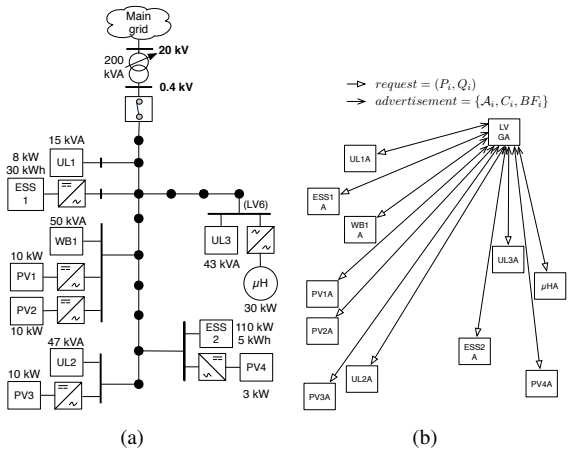

Fig. 1. The electrical network and agents for the case study. (a) Microgrid. (b) Agents. PV: photovoltaic plant. UL: Uncontrollable Load. WB: Water Boiler. ESS: Energy Storage System. μH: micro-hydraulic generator. LVGA: Low-Voltage Grid Agent.

The framework uses a common, device-independent protocol for message exchange between the agents. It hides the specific details of the resources and exposes in an abstract way only the essential information needed for real-time control. In particular, each RA advertises its internal state to its GA using the following three elements.

PQ **Profile and Virtual Cost.** The PQ *profile* of an RA is the region in the (P, Q) plane (for active and reactive power) that the subsystem under the control of this agent can deploy (*negative power means consumption*). The *virtual*

cost function, defined for every (P, Q) in the PQ profile, is interpreted as the cost to this subsystem of applying a requested power setpoint. Its role is to quantify the propensity of this subsystem to deploy (P, Q) setpoints. Note that the cost is virtual and does not represent money.

Belief Function. The *belief function* BF returns the set of all possible (actual) setpoints that the subsystem under RA control *might* implement. Specifically, assuming that the resource receives from its GA a request to implement a setpoint (P, Q), the *actual* setpoint (P', Q') that this subsystem does implement lies in the set $BF(P, Q)$ with overwhelming probability. The belief function accounts for the uncertainty in subsystem operation. In particular, highly controllable subsystems, such as batteries and generators, are expected to have (almost) ideal beliefs, namely $BF(P, Q) = \{(P, Q)\}$. For subsystems such as PV/wind farms, or loads, the belief function will return larger sets, to account for their volatility.

At every time step, a given GA receives the following information: (i) the advertisement messages received from its resources (with PQ profiles, virtual costs, and belief functions), (ii) the power setpoint request obtained from a higher level GA, and (iii) the estimation of the current electrical state of the grid (using real-time methods as in [5], [9]). The goal of the GA is to steer the electrical state of its grid by explicitly setting the power setpoints so that (i) the virtual costs of its resources are minimized, (ii) the power setpoint request from a higher level grid is satisfied as much as possible and that (iii) the grid is in a *feasible state of operation*. The latter refers to *static* (rather than dynamic) feasibility, defined in terms of the nodal voltage magnitudes and line currents, as in [1]. We note that this static analysis is reasonable as we focus on microgrids with little or no inertia, with resources connected to the grid by power electronic interfaces. The process is repeated periodically every 100ms, a value short enough to cope with the fastest possible volatility of distributed resources and large enough to be compatible with the need to estimate the electrical state of the grid.

IV. Unintentional Islanding Maneuver in the Commelec Framework

In this section, we propose a procedure to cope with an unintentional islanding within the Commelec framework. Below is the outline of our method.

(a) At all time, in particular before the islanding event occurs, the GA maintains two lists:
– A rating of all the RAs controlled by the same GA in view of their ability to be a slack resource. This rating is computed based on the power availability and on the state-of-energy (SoE) of each resource. The SoE quantifies the amount of energy that can be withdrawn from a potential slack irrespectively of the PQ profile.
– A list of all the resources (i.e., generators and loads) that have to be shed if the current best candidate slack resource (the first in the previous rating) is selected. This list can be computed from the uncertainty of the resources and an order of shedding priority. We assume the latter is given.
(b) Islanding conditions are continuously monitored via an available real-time state estimation process. When these conditions are detected, the GA sheds all resources in the shedding list and chooses an initial slack based on the current rating.
(c) The grid operation continues during the remainder of the islanding maneuver under the control of the GA as explained in Section III. During this operation, two events can occur:
– The rating of the resources has changed, so that a new slack is selected.
– It is not possible to operate the grid with the current slack (but the rating did not change). In this case, a further load shedding is performed.

We detail the different steps below.

A. Criteria for Selecting the Slack Resources

In this section, we show how the information exchanged between the agents in the Commelec framework can be used to assist in choosing the most appropriate slack resource. In particular, we assume that the GA maintains a rating of all the resources based on (i) the state of energy (SoE) of each resource (in Wh), and (ii) the advertisements from the resource agents. We note that (i) should be sent by the resource agents to the GA, which can be done straightforwardly by adding a message type to the Commelec framework. Also, observe that the knowledge of (i) only is not enough to choose the best appropriate slack. Consider, for example, the case when the grid is *consuming* 10kW and there are two possible slack resources, a battery with SoE=30kWh and a supercapacitor with SoE=2kWh. Without knowing the real-time constraints of these two resources, the natural choice according to the SoE would be the battery. However, if we know (from the advertised PQ profile) that the battery can only supply 5kW whereas the supercapacitor can supply 60kW, we will choose the supercapacitor as the default slack resource (with the possibility to switch later to the battery).

Below we propose a concrete way for preparing this rating. To that end, we introduce additional notation. We let $\mathcal{A}_i \subseteq \mathbb{R}^2$ and $BF_i : \mathcal{A}_i \to 2^{\mathbb{R}^2}$ denote the PQ profile and the belief function of resource i, respectively. We also define the Cartesian product $\mathcal{A} = \mathcal{A}_1 \times ... \times \mathcal{A}_n$, which is the overall PQ profile. The set of all the RAs setpoints is then denoted by $u = (P_1, Q_1, ..., P_n, Q_n) \in \mathcal{A}$, while the set of implemented (actual) setpoints is denoted by $x = (P'_1, Q'_1, ..., P'_n, Q'_n)$. Similarly, we let $BF(u) = BF_1(P_1, Q_1) \times ... \times BF_n(P_n, Q_n)$ denote the overall belief function, so that $x \in BF(u)$ by its definition.

For each candidate slack resource i, and any element (either vector or set) $\mathcal{E}$, we let $\mathcal{E}_{-i}$ denote the same element without considering the resource i. In particular, $\mathcal{A}_{-i} = \mathcal{A}_1 \times ... \times \mathcal{A}_{i-1} \times \mathcal{A}_{i+1} ... \times \mathcal{A}_n$ denotes the overall PQ profile, omitting the PQ profile $\mathcal{A}_i$, and the same for BF_{-i}, u_{-i}, and x_{-i}.

When considering resource i as a slack, we let $Y(x_{-i}|i)$ denote the corresponding electrical state of the grid. Namely, it is the load-flow solution when i is the slack and the power setpoint for other resources is x_{-i}. In the context of radial

distribution networks, it is known that this solution is unique if voltage magnitudes are kept close to nominal values [3]. Similarly, $X_i(x_{-i})$ is the resulting power at the slack bus. The feasibility of the electrical state $Y(x_{-i}|i)$ is defined in terms of the voltage magnitudes and line currents, as in [1]. We denote the set of feasible states when i is the slack by $\mathcal{F}_i$. Finally, we let $\hat{x} = (\hat{P}_1, \hat{Q}_1, ..., \hat{P}_n, \hat{Q}_n)$ denote the current (measured) power setpoint.

We next define the following metrics that are used to rate the candidates for being a slack resource.

1) Controllability of the Resource: We would like to choose resources with no (or little) uncertainty in implementation of the requested setpoint. Recall that the belief function $BF_i(P,Q)$ is the set of all possible power setpoints that resource i may implement when instructed by the GA to do (P,Q). Hence, ideally, we would like to choose a resource with a "perfect" belief function, namely $BF_i(P,Q) = \{(P,Q)\}$. The first metric $\rho_C(i)$ then measures the distance between the perfect belief $\{P,Q\}$ and the advertised one. Formally, we set $\rho_C(i) \triangleq \max_{(P,Q)\in\mathcal{A}_i} \max_{(P',Q')\in BF_i(P,Q)} \frac{d((P,Q),(P',Q'))}{\sqrt{P^2+Q^2}}$, where, $d((P,Q),(P',Q'))$ is the distance imposed by the Euclidean norm. It can be seen that ρ_C is the maximal set-to-set (Hausdorff) distance between the singleton $\{P,Q\}$ and $BF_i(P,Q)$ over all possible $(P,Q) \in \mathcal{A}_i$, measured in percentage relative to the requested setpoint (P,Q). We note that this normalization is essential in order to compare the controllability of resources with different power ratings.

2) Available Power Range: The following metrics measure the ability of resource i to absorb the imbalance in the grid created by the current (measured) setpoint $\hat{x}_{-i}$, taking into account the uncertainties as represented by the advertised belief functions. In particular, let $ABF_i(u_{-i}) \triangleq \{(P_i,Q_i) = X_i(x_{-i}) : x_{-i} \in BF_{-i}(u_{-i})\}$ denote the set of all possible power setpoints that may take place at the connection point of resource i given the uncertainty of all other resources defined by $BF_{-i}(u_{-i})$, or in other words the *aggregated* belief set for the slack power, computed at a given setpoint u_{-i}.

We define the metric $\rho_{P,1}(i)$ to measure the safety margins of resource i as follows: $\rho_{P,1} \triangleq \min_{(P_i,Q_i)\in ABF_i(\hat{x}_{-i})} d\left((P_i,Q_i),\mathcal{A}_i^c\right)$. Here, $\mathcal{A}_i^c$ is the complement of $\mathcal{A}_i$ relative to $\mathbb{R}^2$, and $d(x,S)$ denotes the Euclidean distance of x from the set S. Observe that a positive $\rho_{P,1}$ means that the current setpoint is "safe" in the sense that for any actual implementation, the resulting slack power is feasible. On the other hand, we define $\rho_{P,2}$ as the amount of maximum violation of resource i: $\rho_{P,2} \triangleq \max_{(P_i,Q_i)\in ABF_i(\hat{x}_{-i})} d\left((P_i,Q_i),\mathcal{A}_i\right)$. Note that $\rho_{P,2}$ is positive when the current setpoint may result in a non-feasible actual implementation. We illustrate this idea in Figure 2.

3) Feasibility of the Electrical State: We next define metrics that measure the ability of resource i to provide a feasible electrical state when it is the slack, taking into account the uncertainties represented by the advertised belief functions. Similarly to ABF_i, we let $\mathcal{Y}_i(u_{-i}) \triangleq \{y = Y(x_{-i}|i) : x_{-i} \in BF_{-i}(u_{-i})\}$ denote the set of all possible electrical states that may result from the uncertainty of all resources but i when i is the slack. We then compute the following two distances:

$$\rho_{Y,1} = \min_{y\in\mathcal{Y}_i(\hat{x}_{-i})} d\left(y,\mathcal{F}_i^c\right), \quad \rho_{Y,2} = \max_{y\in\mathcal{Y}_i(\hat{x}_{-i})} d\left(y,\mathcal{F}_i\right),$$

with a similar interpretation to that of $\rho_{P,1}$ and $\rho_{P,2}$. We illustrate this metric in Figure 3.

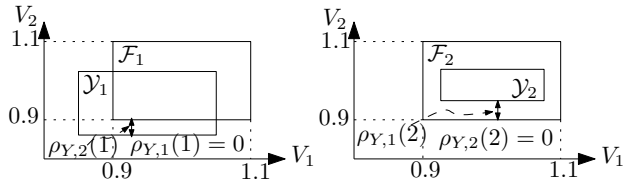

Fig. 3. Illustration of the state-feasibility metric. If the resource $i = 1$ is chosen as slack, it may lead to a non-feasible state ($\rho_{Y,2}(1) > 0$). If the resource $i = 2$ is chosen as slack, it is guaranteed that the state is feasible ($\rho_{Y,1}(2) > 0$). For the simplicity of exposition, the feasibility is defined in terms of the two voltage magnitudes that are required to lie within the interval $[0.9, 1.1]$.

4) Admissibility of Setpoints: As in [1], we consider the set $\mathcal{U}_i$ of *admissible* setpoints when resource i is the slack, that is the collection of target setpoints for all resources but the slack, $u_{-i} \in \mathcal{A}_{-i}$, so that (i) the resulting electrical state is feasible, and (ii) the resulting power at the slack bus fits the PQ profile $\mathcal{A}_i$ of the slack, for any actual implementation that is compatible with the belief functions. Formally, $\mathcal{U}_i$ can be written as $\mathcal{U}_i = \{u_{-i} \in \mathcal{A}_{-i} : \mathcal{Y}_i(u_{-i}) \subseteq \mathcal{F}_i,\ ABF_i(u_{-i}) \subseteq \mathcal{A}_i\}$. Observe that when $\mathcal{U}_i = \emptyset$, it is not possible to operate the grid with the current slack unless a shedding strategy is applied. We thus define a binary metric $\rho_U(i) \triangleq \mathbb{I}\{\mathcal{U}_i = \emptyset\}$, where $\mathbb{I}\{\cdot\}$ is the indicator function. We note that the exact computation of this metric is not feasible in the real-time framework as $\mathcal{U}_i$ is not given explicitly (see [1]). However, a sufficient condition for $\mathcal{U}_i \neq \emptyset$ is that the GA is able to *project* the current setpoint to $\mathcal{U}_i$. As discussed in [1], the GA can use fast *local* projection methods for this purpose, and hence this computation is feasible. In the following, we thus identify the condition $\mathcal{U}_i \neq \emptyset$ with the ability to project to $\mathcal{U}_i$.

5) State of Energy (SoE): Observe that the interpretation of the SoE depends on whether the grid is producing or consuming power. Specifically, given the current setpoint, let $(\tilde{P}_i, \tilde{Q}_i)$ denote the active and reactive power flows at the slack bus assuming that the grid is islanded and i is set to be the slack. We consider a *directional* metric, defined by

$$\rho_E(i) = \begin{cases} (1 - SoE_i)E_{\text{rated},i}, & \text{if } \tilde{P}_i < 0, \\ SoE_i E_{\text{rated},i}, & \text{otherwise,} \end{cases} \quad (1)$$

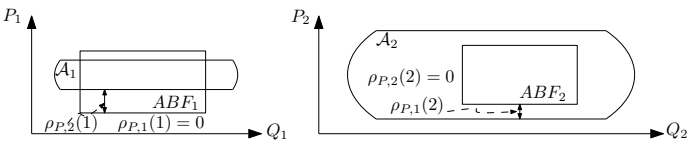

Fig. 2. Illustration of the power availability metric. The case $i = 1$ represents a storage system with low power availability, while the case $i = 2$ represents a storage system with high power availability.

where SoE_i is the state of energy of the resource i (in per unit of the rated power of a given resource), and $E_{\text{rated},i}$ is its rated energy capacity. We note that this metric cannot directly be computed from the information advertised in the original Commelec framework [1], but can readily be obtained by a simple addition to the advertisement messages.

Using $\rho_E(i)$, we also estimate the "survival time" of a slack resource as follows: $\rho_T(i) = \rho_E(i)/\tilde{S}_i$, where $\tilde{S}_i = \sqrt{\tilde{P}_i^2 + \tilde{Q}_i^2}$ denotes the corresponding apparent power.

6) Rating Computation: First, the GA filters out the non-controllable resources and the resources that have too short a survival time, by considering only the set $\mathcal{I} = \{i : \rho_C(i) \leq \epsilon, \rho_T(i) \geq \delta\}$ for some $\epsilon \geq 0$ and $\delta > 0$. The value of ϵ represents the maximum allowed deviation of the actually implemented setpoint from the requested one (in percentage from the requested one). The value of δ is chosen large enough so that the slack can absorb the imbalance during several Commelec cycles. Then, it sorts the resources *lexicographically*, according to

- ρ_U, so that resources with $\rho_U(i) = 0$ (namely, having non-empty set of admissible setpoints) are on top;
- $\rho_{P,2}$ in ascending order, so that resources with the least violation of slack power feasibility are on top;
- $\rho_{Y,2}$ in ascending order, so that resources with the least violation of state feasibility are on top;
- $\rho_{P,1}$ in descending order, so that resources with the maximum power availability are on top;
- $\rho_{Y,1}$ in descending order, so that resources with the maximum state feasibility margins are on top;
- ρ_E in descending order, so that the resources with the highest SoE are on top.

To decide whether two resources i, j have the *same* metric ρ we use an *approximate* equality test, namely $|\rho(i) - \rho(j)| \leq \alpha$ for some small $\alpha \geq 0$. Let $\mathcal{I}(1)$ denote the *best-rated* resource.

B. Computation of Shedding List

First, we assume that the GA has access to a *priority-order list of devices to shed*. This list is used to continuously test the feasibility of the best slack candidate to cope with the unintentional islanding. The priority-ordered list can be computed using the advertised information (e.g., non-controllable resources with large belief functions) and some external information about the criticality of the resources. We consider this order to be *fixed* during the islanding maneuver, and the exact procedure for its computation is out of the scope of this paper. We define now the shedding list $\mathcal{S}$, which is the result of checking the admissibility of the best slack candidate in case the islanded operation takes place. Formally, if shedding is necessary, i.e., if $\rho_U(\mathcal{I}(1)) == 1$, we follow the next procedure:

(a) The first element of the priority-ordered list is added to $\mathcal{S}$.
(b) We recompute $\rho_U(\mathcal{I}(1))$, i.e., the setpoint-admissibility metric of the selected slack $\mathcal{I}(1)$ with this new state of the shedding list.
(c) If $\rho_U(\mathcal{I}(1)) == 0$, we stop, otherwise we add to $\mathcal{S}$ the next element of the priority-ordered list and go back to the previous step. We do this until $\rho_U(\mathcal{I}(1)) == 0$ or the priority-ordered list is exhausted.

C. GA Operation During Islanding Maneuver

Recall that, as the first step, the islanding conditions are detected using real-time state estimation. As a result, the elements of $\mathcal{S}$ are shed and the resource $\mathcal{I}(1)$ is set to be the slack. From that time on, the procedure illustrated in Figure 4 is applied. We note that the condition $\mathcal{U}_{\mathcal{I}(1)} = \emptyset$ can be detected in the "Metric Computation" block *before* the regular decision process of the GA fails to compute the setpoint. This is true because in order to detect this condition, we only need to verify whether it is possible to project to $\mathcal{U}_{\mathcal{I}(1)}$ as discussed in Section IV-A4.

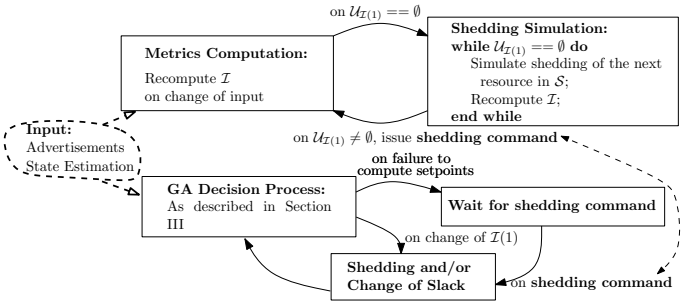

Fig. 4. Illustration of the GA operation during islanding manuever.

V. Performance Evaluation

We compare the performance of the proposed islanding maneuver using the Commelec framework to that of an extended version of the *load drop anticipator technique*. The proposed extension makes this technique able to work with inertia-less systems. The selected case study is shown in Fig. 1; it is based on the CIGRÉ benchmark LV microgrid from [10]. In order to better show the performance of the proposed method, we replaced one uncontrollable load with a high power/low energy storage device (ESS2) that represents a supercapacitor array (SC). We model the behaviour of the SC based on [11].

The islanding is performed at $t = 2$s with the SC as a default slack resource. At this point, the state-of-charge of the array is 25% (corresponding to the SoE of 4.5kWh), which is close to its minimum values. The SC is able to absorb the whole imbalance at this time. At time $t = 4$s, due to the shrinkage of the PQ profile of the SC, the admissible set $\mathcal{U}$ becomes empty. This is shown in Figure 5 that depicts the islanding metrics ρ_U and $\rho_{P,2}$. In particular, $\rho_U = 1$ for the SC at $t = 4$s. Since $\rho_U = 1$ for the battery as well, the shedding of the two loads is performed (UL1 and UL2). As a result, the SC continues to operate as slack until $t = 15$s. At this time, again due to the shrinkage of the PQ profile of the SC, the admissible set becomes empty again, and another load is shed (UL3). As a result both the battery and the SC have non-empty admissible sets ($\rho_U = 0$). However, the power violation is now smaller in the battery ($\rho_{P,2}$ metric in Figure

5), and hence the slack is switched to the battery. As can be seen from Figure 6, the DC voltage and current of the SC are kept within the feasible region during the islanding maneuver. This is achieved in the Commelec framework since the SC agent exposes correctly the internal constraints of the device[1] via the advertised PQ profile. The corresponding AC power profiles of relevant resources are shown in Figure 7. It is worth mentioning that during the maneuver, the GA maintains the QoS of the grid in the feasible set and prevents the SC from being completely depleted. These figures are omitted due to space constraints.

In contrast, in the same scenario, the droop-based technique leads to the violation of the lower bound on DC voltage of the SC in seconds, as shown in Figure 6. In particular, it can be seen in Figure 7 that at around $t = 5.7$s, the SC trips due to this violation, which leads to a failure of the islanding maneuver.

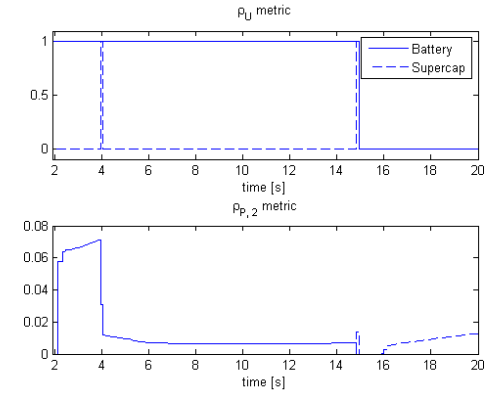

Fig. 5. Relevant islanding metrics.

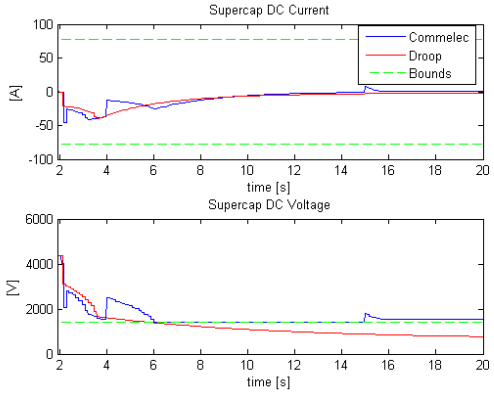

Fig. 6. Supercap DC voltage and current. Dashed green lines represent the upper and lower bounds for the voltage/current. As the upper bound on voltage is much higher than the actual values, it not shown in the graph.

VI. Conclusion

We have proposed a method to cope with the safe unintentional islanding transition of microgrids using the Commelec real-time control framework. Contrary to the standard methods available in the literature, this method is able to choose the best slack resource based on the information obtained from the resource agents, and to switch the slack to a better resource adaptively during the islanding maneuver. Morever, as the GA has a global view of the network's quality-of-supply and its resources, it optimizes the performance of the network during and after the islanding transition. Finally, the method is suitable for inertia-less systems as the control is performed using explicit power setpoints and does not rely on the frequency signal.

[1]To this end, an appropriate SC agent has been developed.

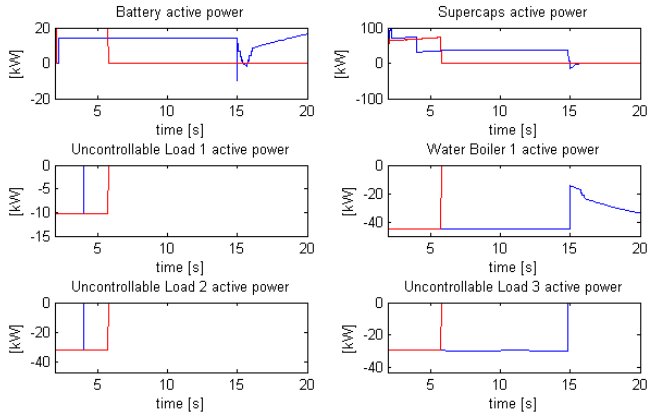

Fig. 7. AC power of different resources.

References

[1] A. Bernstein, L. Reyes-Chamorro, J.-Y. Le Boudec, and M. Paolone. A composable method for real-time control of active distribution networks with explicit power setpoints, 2014. arXiv:1403.2407.

[2] Jeffrey M. Bloemink and M. Reza Iravani. Control of a multiple source microgrid with built-in islanding detection and current limiting. *IEEE Transactions on Power Delivery*, 27(4):2122 – 2132, Oct. 2012.

[3] Hsiao-Dong Chiang and M.E. Baran. On the existence and uniqueness of load flow solution for radial distribution power networks. *IEEE Transactions on Circuits and Systems*, 37(3):410–416, 1990.

[4] T.E. Del Carpio-Huayllas, D.S. Ramos, and R.L. Vasquez-Arnez. Microgrid transition to islanded modes: Conceptual background and simulation procedures aimed at assessing its dynamic performance. In *Proceedings of the 2012 IEEE PES Transmission and Distribution Conference and Exposition (T&D)*.

[5] A. G. Expósito, A. Abur, A. de la Villa Jaén, and C. Gómez-Quiles. A multilevel state estimation paradigm for smart grids. *in Proceedings of the IEEE*, 99(6):952–976, June 2011.

[6] Qiang Fu, AdelNasiri, Vijay Bhavaraju, Ashish Solanki, Tarek Abdallah, and David C. Yu. Transition management of microgrids with high penetration of renewable energy. *IEEE Transactions on Smart Grid*, 5(2):539 – 549, March 2014.

[7] J. A. Peças Lopes, C. L. Moreira, and A. G. Madureira. Defining control strategies for microgrids islanded operation. *IEEE Transactions on Power Systems*, 21(2):916–924, 2006.

[8] R. Palma, C. Benavides, F. Lanas, B. Severino, L. Reyes, J. Llanos, and D. Saez. A microgrid energy management system based on the rolling horizon strategy. *IEEE Transactions on Smart Grid*, 4(2):996 – 1006, May 2013.

[9] M. Paolone, M. Pignati, P. Romano, S. Sarri, L. Zanni, and R. Cherkaoui. A hardware-in-the-loop test platform for the real-time state estimation of active distribution networks using phasor measurement units. *Proceedings of the CIGRE SC C6 Colloquium in Yokohama, Japan, October 6-9, 2013*.

[10] S. Papathanassiou, N. Hatziargyriou, and K. Strunz. A benchmark low voltage microgrid network. In *Proceedings of the CIGRÉ Symposium "Power Systems with Dispersed Generation: technologies, impacts on development, operation and performances"*, Apr. 2005, Athens, Greece.

[11] D. Torregrossa, M. Bahramipanah, E. Namor, R. Cherkaoui, and M. Paolone. Improvement of dynamic modeling of supercapacitor by residual charge effect estimation. *Industrial Electronics, IEEE Transactions on*, 61(3):1345–1354, March 2014.